JOURNAL OF GEOPHYSICAL RESEARCH, VOL. 112, D09107, doi:10.1029/2005JD006420, 2007

Origin and transport of tropical cirrus clouds observed over Paramaribo, Suriname (5.8°N, 55.2°W)

J. P. F. Fortuin,[1,2,3] C. R. Becker,[4] M. Fujiwara,[5] F. Immler,[6] H. M. Kelder,[1,2] M. P. Scheele,[1] O. Schrems,[6] and G. H. L. Verver[1]

Received 28 June 2005; revised 19 April 2006; accepted 29 August 2006; published 8 May 2007.

[1] The Intertropical Convergence Zone (ITCZ) passes twice a year over tropical Suriname, bringing two wet and two dry seasons. During a pilot study campaign in Suriname, cirrus clouds were observed with a mobile aerosol Raman lidar (MARL) and with balloon sondes containing a frost point hygrometer called Snow White, over the period October–November 2004. These observations are used to study the origin of cirrus clouds and the dynamical processes that determine their transport, using European Centre for Medium-Range Weather Forecasts (ECMWF) operational analyses. The height of cirrus occurrence is in phase with the height of the cold point tropopause, with maximum heights occurring during Northern Hemisphere winter that are about 2 km above the minimum values in summertime. The occurrence of cirrus often corresponds with a northerly meridional wind flow (in a layer underneath the tropopause), also when the ITCZ lies to the south in the period January–May. ECMWF analyses point out that inertial instability flow, in the form of vertically stacked meridional circulation cells in the upper troposphere (UT), can explain the transport of these cirrus events. Also evident is that radiative cooling of a moist layer transported in the UT leads to a thermal wind in the form of an easterly/westerly jet associated with the southward/northward transport of moist air. An interactive play between the inertial instability and thermal wind mechanisms explains many of the observed features of cirrus occurrence over Suriname. The observed cirrus mostly originates from the ITCZ or from deep convective centers to the south that form during the early summer monsoon.

Citation: Fortuin, J. P. F., C. R. Becker, M. Fujiwara, F. Immler, H. M. Kelder, M. P. Scheele, O. Schrems, and G. H. L. Verver (2007), Origin and transport of tropical cirrus clouds observed over Paramaribo, Suriname (5.8°N, 55.2°W), *J. Geophys. Res.*, *112*, D09107, doi:10.1029/2005JD006420.

1. Introduction

[2] The process of cirrus formation in the tropics and its contribution to the water vapor budget of the upper troposphere and lower stratosphere (UTLS) are still not fully understood. These topics have received more attention in view of an observed increase in stratospheric water vapor over the last decades, paradoxically against a steady decrease of tropical tropopause temperature of about 0.5 K/decade [*Seidel et al.*, 2001]. Satellite and balloon observations however show a sudden drop in stratospheric water vapor beginning in 2001, accompanied by a colder tropical tropopause with lower ozone values, which points again to tropopause-controlled humidity and an increase in tropical upwelling since 2001 (W. J. Randel, personal communication, 2005). Changes in upper tropospheric water vapor (UTWV) and cirrus can strongly affect climate forcing, and also cause changes in the UTLS ozone chemistry. Using satellite microwave observations of UTWV and infrared observations of cirrus in the tropics, *Luo and Rossow* [2004] found that cirrus clouds can last for one to two days, enough to be advected horizontally over a distance of 600–1000 km. They point out that the lifetime of cirrus far exceeds the lifetime of individual cirrus particles, which means that there must be a large-scale replenishment and lifting of moisture to support growth of new cirrus particles. They found that at least half of all tropical cirrus clouds are formed in situ, away from the cumulonimbus detrainment area. Typically, a decaying cumulonimbus spawns cirrostratus as well as cirrus; the former normally decays quite rapidly whereas the latter can continue to grow and then gradually gets thinner in time. Cirrus is not necessarily the cause of a moister upper troposphere (UT), as they found that the UT is often moist before and after cirrus has formed in the layer. The role of cirrus on ambient moisture is thought to be largely dependent on the microphysics involved: homogeneous nucleation

[1]Royal Netherlands Meteorological Institute, De Bilt, Netherlands.
[2]Formerly at Technical University of Eindhoven, Netherlands.
[3]Now at Road and Hydraulics Engineering Institute of the Netherlands Public Works Department, Netherlands.
[4]Meteorological Service of Suriname, Suriname.
[5]Hokkaido University, Sapporo, Japan.
[6]Alfred Wegener Institute for Polar and Marine Research, Bremerhaven, Germany.

0148-0227/07/2005JD006420$09.00

resulting from slow ascent rates allows high supersaturation (1.2–1.6) of ambient air, whereas heterogeneous nucleation can occur in fast ascending air with lower saturation values [*Jensen et al.*, 2001]. Thus the dehydration potential of cirrus is a function of microphysical parameters like particle size, number density and residence time of air in the cloud. Recent observations of cirrus near the tropical tropopause do however show that saturation ratios of 1.2–1.3 are maintained also within cirrus that have extensive ice surface areas [*Jensen and Pfister*, 2005], challenging the idea that crystal growth depletes ambient water vapor given enough time.

[3] *Fueglistaler et al.* [2004] studied troposphere to stratosphere (TST) exchange in the tropics using forward and back trajectories from analyses of the European Centre for Medium-Range Weather Forecasts (ECMWF). They find that air parcels pass through the tropical tropopause layer (TTL) typically within 13 days, before they reach the stratosphere. *Highwood and Hoskins* [1998] defined the TTL as a transition layer directly above the level of most deep convection, and below the level of direct control from extratropical wave driving; the mechanism that drives the Brewer-Dobson circulation in the stratosphere [*Haynes et al.*, 1991]. The bottom of the TTL is often defined as the level of lapse rate change or the level of zero radiative heating (clear sky), which is typically around 13–15 km. Therefore an air parcel released in the TTL experiences positive diabatic heating which causes an ascent into the stratosphere. Two dynamical processes in the UT and TTL will now be discussed that will largely determine the perspective in which the transport of cirrus and moist air in the present study is analyzed: a thermal wind resulting from moist air advection, according to a study of *Fujiwara et al.* [2003a] (henceforth called *Fu03*); and inertial instability flow resulting from negative potential vorticity (PV) zones in the Northern Hemisphere UT, according to a study of *Fortuin et al.* [2003] (hence called *Fo03*).

1.1. Thermal Wind Resulting From Moist Air Advection

[4] From shipborne radiosonde measurements performed in the tropical East Pacific, *Fu03* detected a recurring upper tropospheric inversion (UTI), which they suggest is a climatological feature that often constitutes the TTL bottom. The UTI seemed to be caused by radiative cooling of a very humid outflow layer that was advected southward from the Intertropical Convergence Zone (ITCZ) to the north at about 10°N. They found that a north–south temperature gradient is established as the cooling moist layer journeys southward, creating an easterly jet that is in thermal wind balance with the temperature gradient. The easterly jet again spreads the inversion downstream along the equator, such that it becomes a widespread feature in the tropics. One can argue that the thermal wind balance requires geostrophic flow, which does not happen near the equator where the Coriolis parameter becomes zero. *Fu03* however showed that this is compensated by the fact that the vertical wind shear is also inversely proportional to Coriolis, thus creating a strongly enhanced effect near the equator.

1.2. Inertial Instability Flow in the UT

[5] In an opposite situation, with the ITCZ to the south near the equator and moist air now being transported northward along with the Hadley cell, *Fo03* found that the occurrence of inertial unstable conditions in the UT above Suriname can lead to the formation of a meridional circulation cell situated directly above the Hadley cell. This subcell has the same horizontal extent as the Hadley cell and conforms in shape to the vertically stacked circulation cells predicted from inertial instability theory under zonal symmetric conditions [*Dunkerton*, 1981]. Although theory also predicts maximum growth rates for infinitely small vertical wavelengths, *Fo03* showed that viscosity values typical for the UT allow maximal growth at the observed vertical wavelength, and thus dampen out flow on smaller scales. *Hitchman et al.* [1987] confirmed the existence of such cells by detecting alternating temperature extrema (caused by divergence/convergence of flow at the cell outer ends) in the equatorial lower mesosphere; a so-called "pancake structure". In their analysis, *Fo03* found from ECMWF analyses that the upper subcell transports moist air southward again, after it has branched upward from the Hadley cell into the TTL. In the current study we show that cirrus clouds are transported along with this southward flow, caused by condensation during the ascent from the Hadley cell below.

[6] In the present study, cirrus detected over Paramaribo station with the balloon-flown frost point hygrometer sensor Snow White is analyzed with respect to its origin and transport dynamics, with a focus on the transport mechanisms presented in *Fu03* and *Fo03*. Section 2 describes the Paramaribo station data used for the current analysis, as well as some climatological features of the station. Section 3 presents the observation results in relation to ECMWF analysis fields, followed by a detailed analysis in section 4 and conclusions in section 5.

2. Observations

[7] Intensive observations started at Paramaribo station in 1999, along with weekly ozone- and radiosonde balloon launches. The station lies in the southwestern outskirts of Paramaribo, the capital of Suriname, which is still in a relatively pristine environment as the Atlantic Ocean lies to the north and the Amazon forest stretches southward, from the outer perimeters of the city up to and beyond the inland borders of the country. In September 2002 a receiving station for the balloon-launched Snow White frost point hygrometer was installed, and since then 37 launches with the Snow White have been performed. The Snow White hygrometer can perform accurate water vapor measurements in the upper tropical troposphere, where the regular Vaisala humicap sensors start to fail as their response to humidity changes becomes very slow at such low temperatures. The lower detection limit of the Snow White is 2–6%; the uncertainty depends on the temperature and humidity itself. More detailed analyses of the Snow White measurement technique, performance and accuracy can be found in *Fujiwara et al.* [2003b], *Vömel et al.* [2003] and *Verver et al.* [2006]. Table 1 gives the Snow White launch dates and times of the first 28 launches, and an indication of the height at which cirrus ('=') or an almost saturated layer ('-') was detected. Cirrus is defined here to occur when (super)saturation with respect to ice is measured by the Snow White in the UT. When the household signals from the Snow White (i.e., the current of the Peltier element,

Table 1. Launch Dates and Times of Snow White Hygrometer Sondes, Along With Season (Wet or Dry), Concurrent Observations, and Markings of the Height at Which Cirrus or Very Moist Layers were detected[a]

					Height of Cirrus, km									
Season	Number	Date	Time GMT	Concurrent Observation	10	11	12	13	14	15	16	17	18	19
Long dry (ITCZ to north)	1	16 Oct 2002	23:00	O_3, V				=					-	
	2	17 Oct 2002	22:20		=	==	=	===					-	
	3	18 Oct 2002	22:20			-		–	-				-	
	4	22 Oct 2002	22:20				-		–				=	
	5	23 Oct 2002	22:15	~O_3, ~V				=	==	=		==		
Short wet	6	28 Jan 2003	22:25	O_3, V					defect					
Short dry (ITCZ to south)	7	28 Feb 2003	22:50				-	=	=	=	=	=	?	=
	8	31 Mar 2003	23:00				==	==	===		=		=	
Long wet	9	30 Apr 2003	23:00								-		=	
	10	30 May 2003	22:55			-	==	==		-		==		
	11	30 Jun 2003	22:35			=	=	=	=					
Short dry (ITCZ to north)	12	11 Feb 2004	22:30			-				defect				
	13	18 Feb 2004	22:30				-	=	==	=		===		
	14	25 Feb 2004	22:55		–	–			—	=	=	==	=	
	15	10 Mar 2004	22:30		–			–	—		—	–		
	16	17 Mar 2004	22:30		–				-	=		—		—
Long dry (ITCZ to north)	17	15 Oct 2004	6:45	O_3, lidar			=	==	=	=-	=	=	==	?
	18	21 Oct 2004	7:45	lidar	=		==	==	==	==	==	?		
	19	27 Oct 2004	6:45	O_3, V	–			–						
	20	31 Oct 2004	6:30	O_3, V, lidar	–	=	===	=		—				
	21	3 Nov 2004	5:50	lidar			=		=					
	22	6 Nov 2004	6:35	lidar	-			==					–	-
	23	9 Nov 2004	6:20	O_3, V, lidar		=		=	-	==	=			
	24	10 Nov 2004	6:30	lidar				=		==				
	25	12 Nov 2004	6:45	lidar						=				
	26	15 Nov 2004	6:35	~lidar	–	–	-	==						=
	27	16 Nov 2004	6:25	V, lidar	=						==	–		
	28	22 Nov 2004	6:25	O_3, V, lidar				==	==	==			=	-

[a]The quality of the Snow White signal is questioned if an '?' is added to the marking (see text). Concurrent Observations: O_3 = ozonesonde, V = GPS wind fields, lidar = concurrent lidar backscatter profiles. Cirrus is indicated with '='; very moist layers are indicated with '-'. In the last column the height scale ranges from 10 to 19 km in an analog way, each height mark corresponding with the middle of the two numbers (e.g., 10 km mark between "1" and "0"). ITCZ: Intertropical Convergence Zone.

phototransistor voltage, etc.) indicated technical limiting or malfunctioning conditions, a question mark is added to the moisture or cirrus indicators of Table 1. Relevant concurrent observations performed during the launches are also indicated. The last 12 launches listed in Table 1 were part of a pilot study observation campaign, during which a mobile aerosol Raman lidar (MARL, from the Alfred Wegener Institute in Bremerhaven) was tested on its suitability for long-term deployment in the tropics. The MARL system is capable of detecting even extremely thin ice clouds at the tropical tropopause [*Immler and Schrems*, 2002]. All launches were performed in the dark, as night-type Snow Whites were used that minimize potential contamination and do not suffer from solar radiative heating. Coincidentally, the lidar also performed best at night as the receptor unit tended to overheat during daytime.

[8] The launch dates in Table 1 are categorized into seasons following a climatological subdivision for Paramaribo: the long dry season when the ITCZ is to the north and southeasterly trade winds are blowing (August–November), a brief wet season (December–January) when the ITCZ is overhead, followed by a short dry season with northeasterly trade winds (February–March) and the ITCZ near the equator, and finally a long wet season (April–July) when the ITCZ migrates gradually northward over Suriname. These transitions can also be detected from balloon sonde observations in Figure 1, showing height-time cross sections of the annual cycle in humidity, temperature, wind and ozone; averaged in week bins over the period January 2000 to December 2004. Note that the water vapor field in Figure 1a is derived from Vaisala humicap sensors (RS80A or H radiosonde), which are not reliable above 11 km [*Verver et al.*, 2006]. The tropopause is indicated with a black line in Figure 1, and corresponds with the minimum temperature as can be seen in Figure 1b. Temperature lapse rates (equal to dT/dz [K/km] in this paper) are shown in Figure 1c, with minimum values occurring in a broad layer from 10–14 km, above which the lapse rate increases again, reaching positive values above the tropopause.

[9] Figure 1a shows a systematic increase in lower-tropospheric humidity when the southeasterly trade wind near the surface switches to northeasterly in early December (Figure 1e, indicated with an "A"), marking the onset of the short wet season from December–January when the ITCZ reaches the Suriname coast. The ITCZ then rapidly progresses to a summer thermal low created inland over the Amazon inland, which brings the short dry season to Suriname from February–March when the ITCZ reaches its southernmost excursion over the equator. Then a long wet season April–July follows as the ITCZ retreats northward, more slowly this time as it is now in step with the ITCZ to the east over the Atlantic Ocean where sea surface

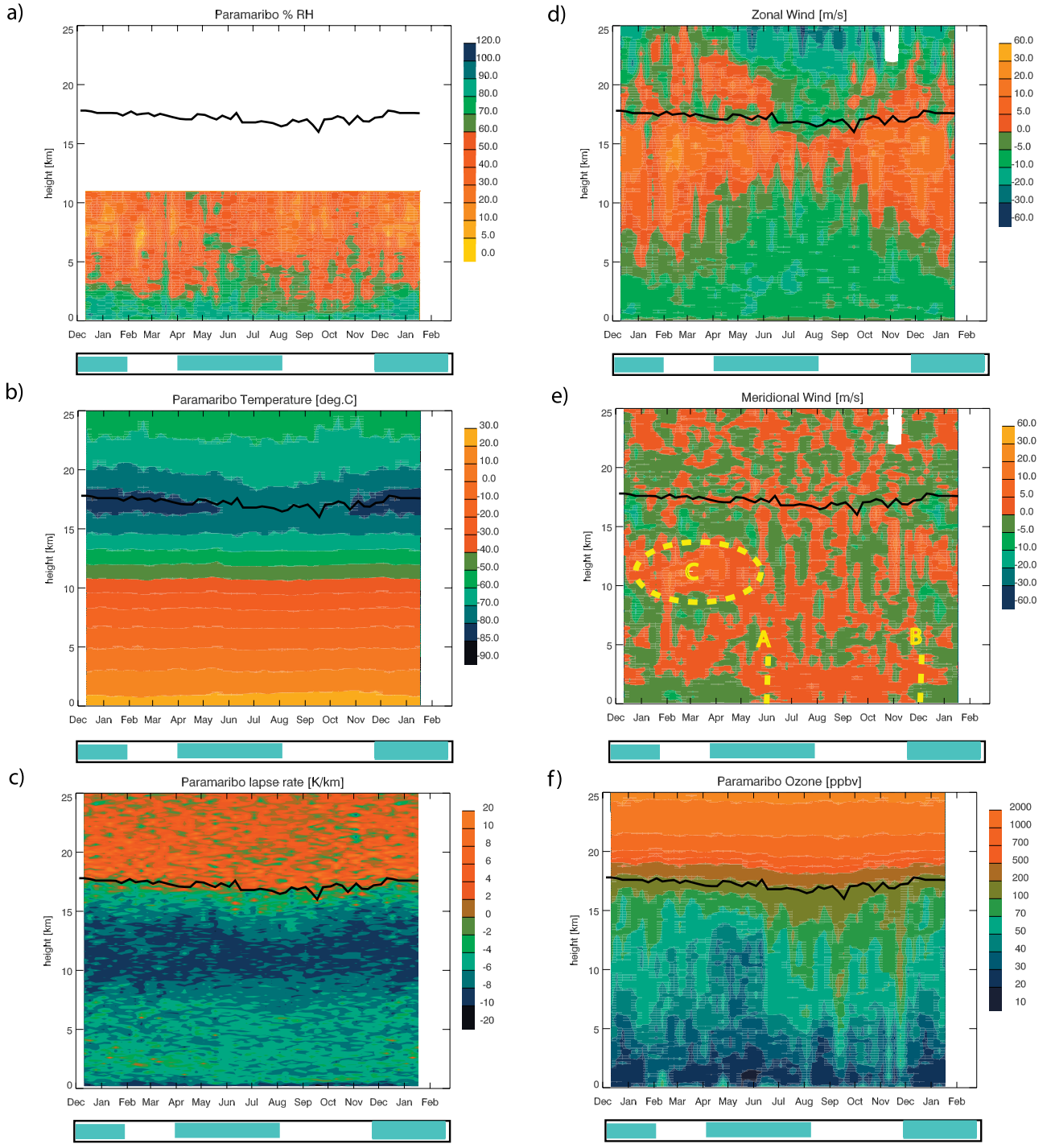

Figure 1. The annual average cycle (weekly averages) versus height from Paramaribo sonde observations over the period January 2000 to December 2004 for (a) relative humidity, (b) temperature, (c) lapse rate in K/km, (d) zonal wind, (e) meridional wind, and (f) ozone volume mixing ratio. The climatological wet and dry seasons of Paramaribo are indicated with blue and white, respectively, in the bar below the x axes; the Intertropical Convergence Zone (ITCZ) lies to the south of Paramaribo for the period between "A" and "B" of Figure 1e.

temperatures are highest. The switch back from northeasterly to southeasterly trade winds beginning June (Figure 1e, indicated with a "B") marks the last stage of this long rainy season. The ozone field of Figure 1f mirrors the wet and dry seasonality; as low ozone values from the boundary layer are transported upward by deep convection during the rainy seasons, replacing the higher ozone values that dominate the UT. During the monsoon period (northeasterly trade winds over Suriname) westerly winds dominate in the UT (Figure 1d) as the subtropical jet is then closer to the equator because of the stronger latitudinal temperature gradient during the NH winter. Also evident in this period is the

Hadley circulation, when the northeasterly trade winds at the surface are balanced by southerly flow above in a layer from 10–14 km (Figure 1e, marked with a "C"), which roughly corresponds in altitude with the minimum lapse rate layer mentioned earlier (Figure 1c). The NH winter corresponds with an intensified Brewer-Dobson circulation, and a higher and colder tropopause above Paramaribo (Figure 1b). The preceding description is still a simplified and localized view of the monsoon cycle, and attention will be given to other characterizations of the circulation pattern in the analysis of section 4.

3. Results

[10] The Snow White observations are now compared with ECMWF operational analyses, as section 4 will largely resort to these analyses to infer the origin and transport dynamics associated with observed cirrus clouds. Figure 2 shows height-time cross sections of relative humidity, according to Snow White observations (Figures 2a–2c) on the dates listed in Table 1, and the corresponding ECMWF operational analyses (Figures 2d–2f) at 12:00 GMT. The spatial resolution of the ECMWF analyses for the horizontal is about 40 × 40 km (T511) and for the vertical about 1 km in the UT. The relative humidity is calculated with respect to liquid water if ambient temperature is above freezing point, otherwise with respect to ice according to *Hyland and Wexler* [1983]. Please note that the data are interpolated between the launch dates, giving the contour plots a horizontally stretched look. Three different periods are considered, arranged according to observation intensives or according to seasonality. Particular attention is given to the pilot study campaign period mentioned earlier (compare with Figure 3), as this is the period most supported by independent and complementary measurements. Figures 3a–3e show Snow White and other radiosonde observations, along with the corresponding daily ECMWF analyses at 7:00 GMT, in Figures 3f–3j.

[11] Most noticeable from the comparison in Figures 2 and 3 is that ECMWF humidity misses the fine-scale structure of Snow White, especially higher up in the UT, but that for several instances the agreement is quite good. Also for the other radiosonde parameters in Figure 3 one can see good agreements with the analyses, especially for temperature and wind. Note however that the additional observations were not always performed simultaneously to the Snow White launches, so they are presented on different time intervals and are now compared with daily ECMWF fields.

[12] As mentioned in section 2, lidar backscatter and Raman observations were performed often concurrent to Snow White launches. A cirrus event is defined in this study to occur for Snow White or ECMWF values that are (super)saturated with respect to ice in the UT. *Heymsfield et al.* [1998] found that ice (super)saturation is a necessary but often not sufficient requirement for cirrus to form. *Immler et al.* [2007] on the other hand found that the cirrus events detected by lidar during the same campaign in Suriname (compare with Figure 4) compare very well with the Snow White ice saturated fields as well as with ECMWF cloudiness data. Their analysis suggests that high supersaturation is not necessary for cloud formation in the TTL, thus indicating that ice saturation is quite a good proxy for cirrus occurrence. This should also be the case for ECMWF ice saturation values, as the humidity is calculated over a grid box now (40 × 40 × 1 km), which enhances the chances that cirrus will occur somewhere in this saturated grid box (Figure 3a versus Figure 3f). Differences between Figure 4 (top) and Figure 4 (bottom) can sometimes also be attributed to localized cirrus events, on the occasions when the balloon drifted too far from the lidar beam to observe the same event. Even though this drift was found never to be beyond 0.3 degrees in longitude or 0.1 degree in latitude (derived from GPS signals used for wind) from the laser beam in the troposphere, this was enough to bypass a few localized cirrus clouds detected by lidar.

4. Analysis

[13] It was shown in the previous section that there is a reasonable agreement between ECMWF operational analyses on the one hand and Snow White (and lidar) observations on the other. Of course the ECMWF fields in Figures 2 and 3 have a coarser structure (due to the model layering) than the observed fields. It seems that an averaging of the humidity observations over the same layer thicknesses as ECMWF would produce slightly lower layer humidity averages and thus indicate a small wet bias in the ECMWF tropical upper troposphere. However, there are also occasions where observed humidity is higher than ECMWF humidity and on quite a few instances essential individual features like the height and thickness of detected cirrus events are well simulated by ECMWF. Therefore this section will resort mainly to ECMWF analysis fields to determine the origin, transport and dynamics of cirrus in the UT. This is first done by assessing the possible contribution of the dynamical processes proposed by *Fu03* and *Fo03*, as discussed earlier in the introduction. These analyses are then put against the climatological circulation patterns typically encountered over South America. Finally, ECMWF back-trajectories are calculated starting from observed cirrus events, and interpreted in terms of earlier analyses.

4.1. Dynamical Processes

[14] Similar to Figure 1, the annual cycle of humidity, temperature, lapse rate and wind versus height is shown in Figure 5, averaged over the same period, January 2000 to December 2004, but now for daily ECMWF operational analyses at Paramaribo coordinates. The temporal variability of the plots clearly differs, as Figure 5 shows daily averages versus the weekly averages in Figure 1. Another difference lies in the humidity fields, as Figure 1a shows Vaisala humicap observations that are unreliable above 11 km. For the rest, a good agreement can be seen, especially for the temperature and wind fields. A striking feature of the humidity field in Figure 5a is the annual cycle in cirrus height. The highest cirrus clouds occur after the onset of the South American Summer Monsoon (SASM) around January–March, when they are about 2 km higher than the cirrus encountered toward the end of SASM in June–July. Although there are too few Snow White profiles to confirm this feature statistically (particularly toward the end of SASM), Table 1 does indicate a similar relation of cirrus height versus time of year. As a rough indication, averaging the heights of ice saturation occurring in Table 1,

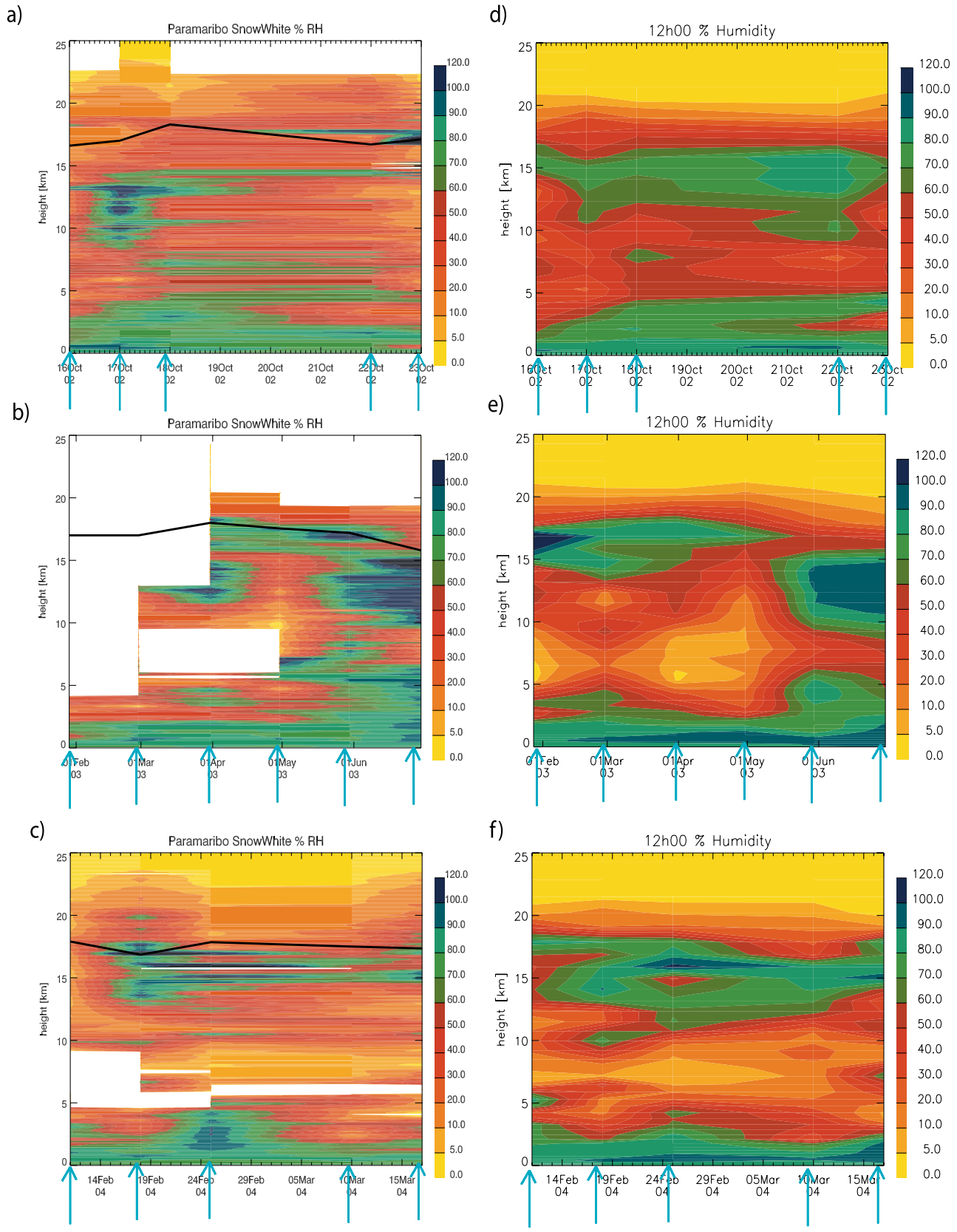

Figure 2. Height-time cross sections from (a–c) sonde observations and (d–f) European Centre for Medium-Range Weather Forecasts (ECMWF) operational analyses showing relative humidity with respect to water (T > 0°C) or ice (when T < 0°C). Data between the launch dates (indicated with blue arrows; see also Table 1) are interpolated for both radiosonde and ECMWF fields. Note that the x axes are over different timescales for the top, center, and bottom pairs.

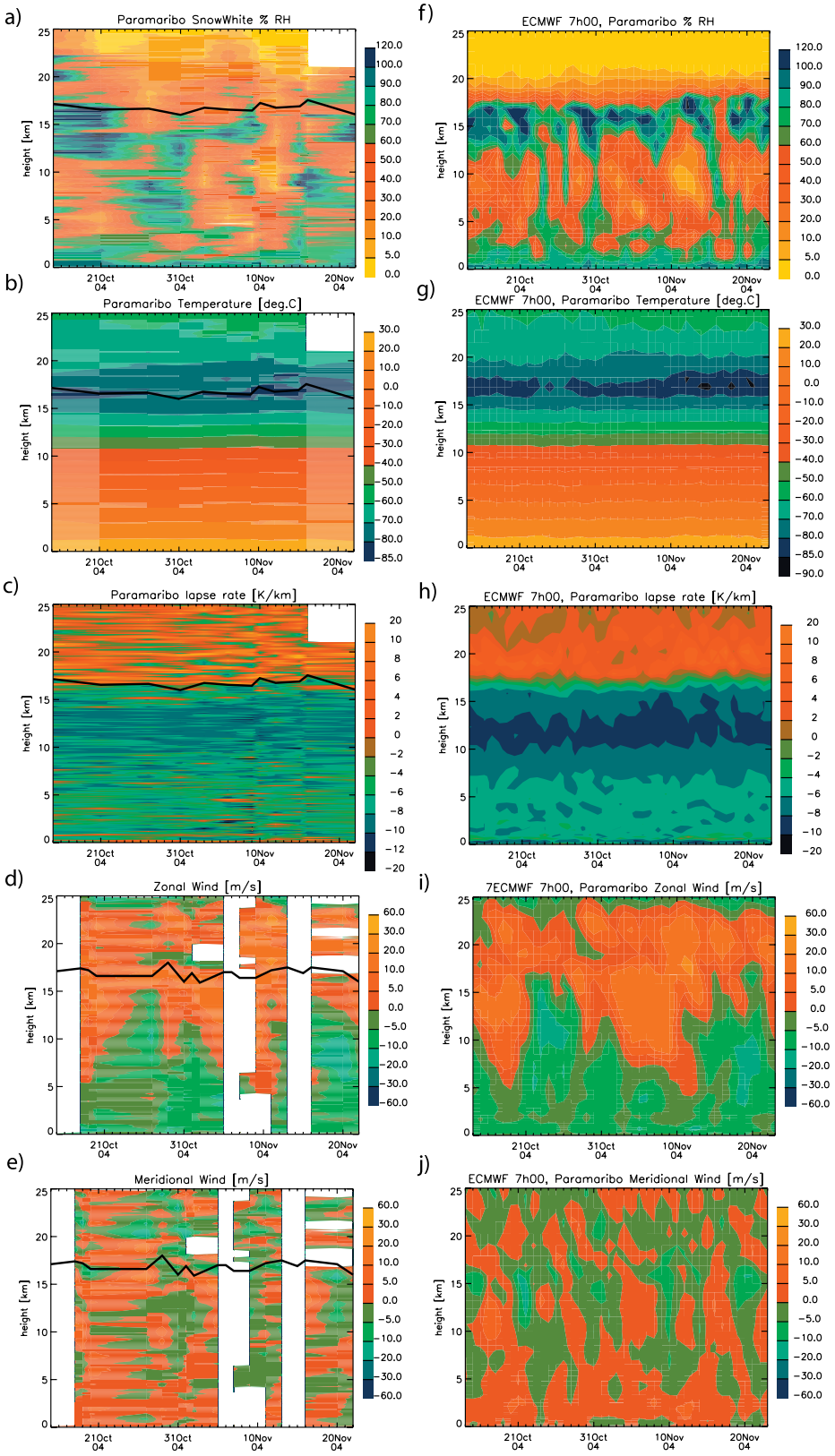

Figure 3. Height-time cross sections of (a–e) radiosonde observations and (f–j) corresponding ECMWF operational analyses showing Snow White and ECMWF relative humidity (Figures 3a and 3f), temperature (Figures 3b and 3g), lapse rate in K/km (Figures 3c and 3h), zonal wind (Figures 3d and 3i), and meridional wind (Figures 3e and 3j). Relative humidity is with respect to water ($T > 0°C$) or ice (when $T < 0°C$). The sonde data are interpolated between launch dates (compare with Table 1), whereas daily ECMWF fields are shown.

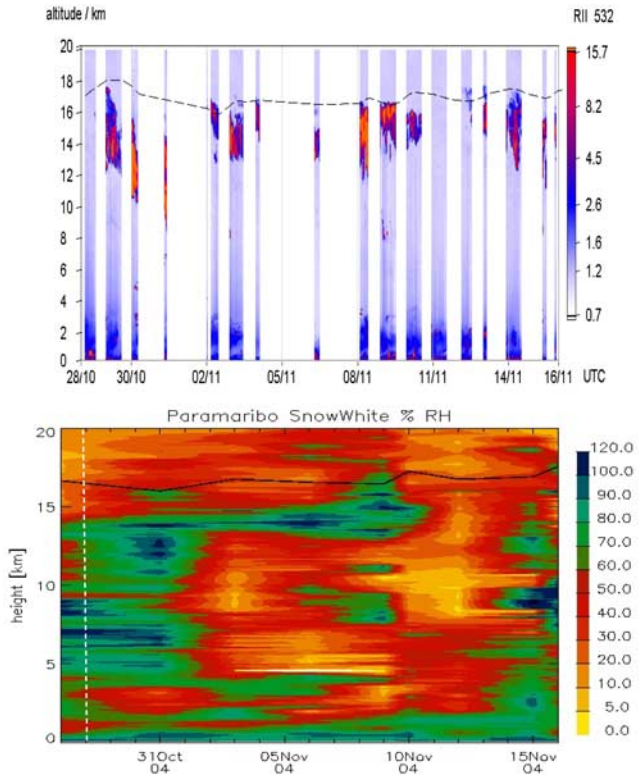

Figure 4. Lidar height-time cross section of the backscatter ratio at 532 nm (top) and Snow White relative humidity (bottom), measured at Paramaribo from 28 October 2004 to 16 November 2004 (comparable with the period in Figures 3a and 3f). White areas indicate episodes when no lidar data are available. The cold point tropopause is indicated with a black dashed line (Figure 4, top) and solid line (Figure 4, bottom).

gives a 13.6–16.7 km height range during the short dry season in early SASM (February–March), versus a range of 12.2–15.5 km during the long dry season after SASM. A straightforward explanation can be found in the temperature field of Figure 5b, showing a colder and higher tropopause in January compared to July (which again can be related to the intensified Brewer-Dobson circulation in NH winter); and hence lower saturation values over ice which enhances cirrus formation.

[15] A closer inspection also reveals that occurring cirrus almost always coincides with a northerly component in the meridional wind, as can be seen from Figure 5e. The thin white contour lines in Figure 5e corresponds with the 80% humidity contour line (Figure 5a), thus indicating that around 15 km the higher than 80% humidity values correspond with southward flow (green color Figure 5e). This is to be expected when the ITCZ lies to the north of Paramaribo, when moist air detrained from deep convection in the ITCZ travels southward; but seems surprising when the ITCZ lies to the south and moist air is transported by southerly winds along with the Hadley cell. This northward transport is even clearly visible in Figure 5e between 10 and 14 km during December–June, but the cirrus (or high relative humidity) events mostly occur above this layer where southward transport dominates. As mentioned earlier in the introduction, *Fo03* argued that this southward transport close to the tropopause is a consequence of inertial instability, for which the conditions (a negative potential vorticity, indicated with black contour lines in Figure 5) often occur in the UT during SASM. Hence a subcell situated on top of the Hadley cell would cause the southward flow directly underneath the tropopause, driven by inertial instability, as depicted schematically in Figure 6. In the UT, the subtropical jet (STJ) then migrates equatorward during NH winter, causing a strong relative vorticity (mainly $-\partial u/\partial y$) that exceeds the planetary vorticity f, and thus creating a negative absolute vorticity ($\eta = \zeta + f$) zone in the UT directly north of the equator. ECMWF analyses learn that also the potential vorticity ($PV = -\eta\, g\, \partial\theta/\partial p$) becomes negative in this region of the UT, indicating that this air is advected across the equator from the Southern Hemisphere. *Sato and Dunkerton* [2002] first reported the regular occurrence of negative PV in the UT over Japan, and showed through trajectory calculations that these events are thin layered cross-equatorial excursions coming from the Southern Hemisphere. The dominant westerly winds in the UT during the monsoon (Figure 5d, above 10 km for December–June) testify to the STJ's influence, and we see that negative PV values prevail in this period at the height of the outflow layer (Figures 5d and 5e, black contour lines). To alleviate the resulting instability, meridional flow will transport easterly momentum from the equator northward (upper branch Hadley cell) and westerly momentum from the STJ southward (subcell beneath tropopause). This mechanism therefore seems to play an important role in driving the Hadley cell and also establishing the height of the upper return flow at the height of the STJ. Following this argument, moist outflow from deep convection over the Amazon is then transported northward over Suriname, but only crystallizes to form cirrus when it is tilled to a higher level by the subcell directly above to flow southward again underneath the tropopause; as depicted schematically in Figure 6.

[16] A particular case study on 1 April 2003 gives a similar view, as shown in Figure 7 for height-latitude cross sections along Paramaribo longitude 55°W. The westerly zonal winds above 100 hPa in the tropics indicate that the QBO westerly phase is descending toward the tropopause in this period. The horizontal zonal wind shear south of the STJ (Figure 7a, indicated with an "A") corresponds with a negative PV field in the UT (Figure 7b, also "A") and a region of northward flow around 200 hPa, with southward flow above it (Figure 7c, "A"). As mentioned earlier, this PV structure is evidence of Southern Hemisphere air advected northward at about 200 hPa (and consequent upward and southward flow due to the vertically stacked cell above the Hadley cell). These northward and southward velocities both have maximum values between the equator and the edge of the negative PV domain, as is predicted from theory. The relative humidity field in Figure 7d shows deep convection of the ITCZ directly south of the equator, as well as northward outflow of moist but unsaturated air around 200 hPa, reaching saturation higher up in the return flow around 100 hPa. Also, one can see southward/northward transport of westerly/easterly momentum at 100 hPa/200 hPa. In *Fo03* a similar situation is found for an averaged period over 10 days (February–March 2003),

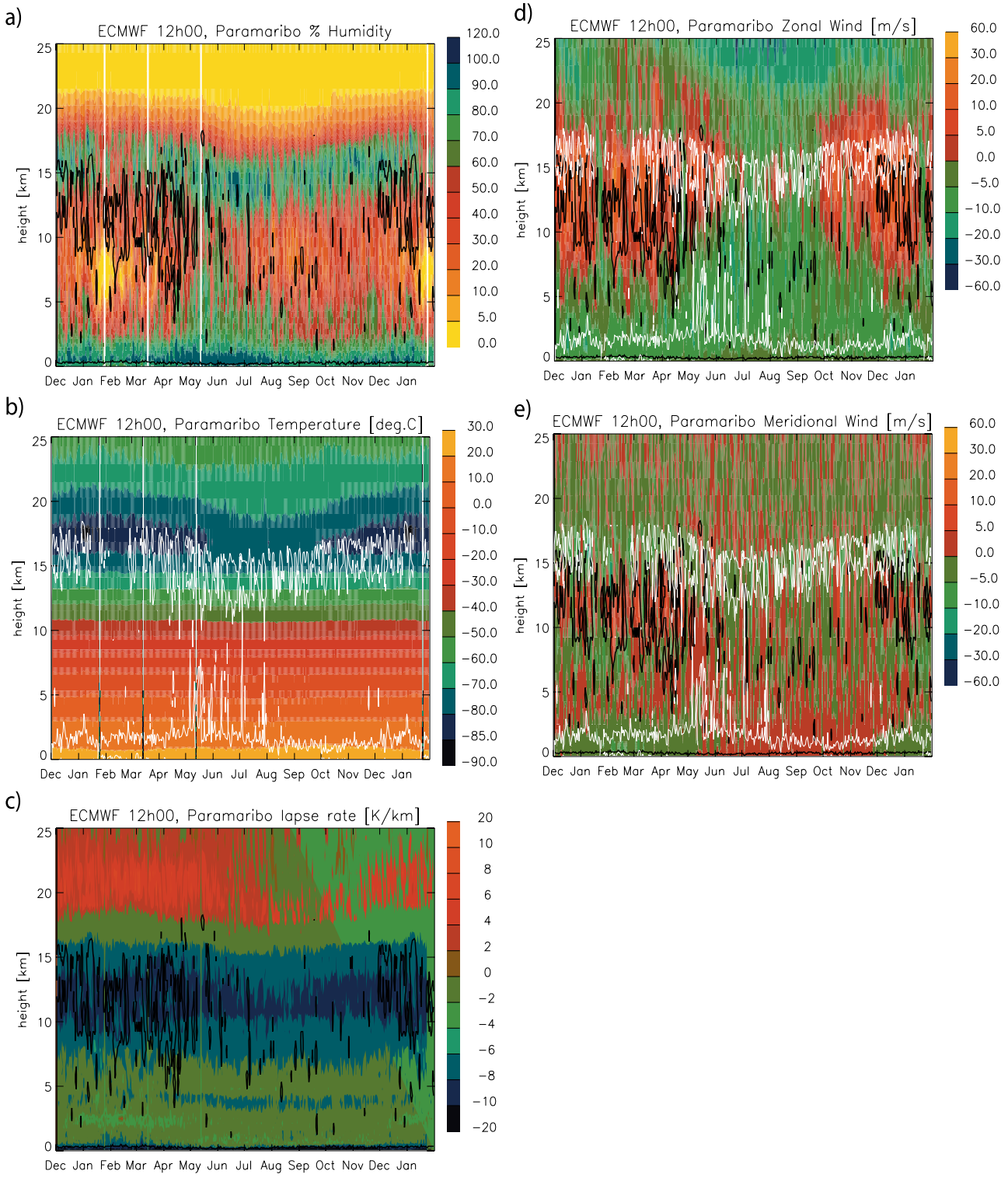

Figure 5. The annual average cycle (daily averages) versus height from ECMWF operational analyses over the period January 2000 to December 2004 for relative humidity (a), temperature (b), lapse rate in K/km (c), zonal wind (d), and meridional wind (e). Black contour lines indicate zero potential vorticity (PV) (negative within closed loop); the white contour lines (b, d, and e) correspond with 80% humidity over ice or water (derived from Figure 5a).

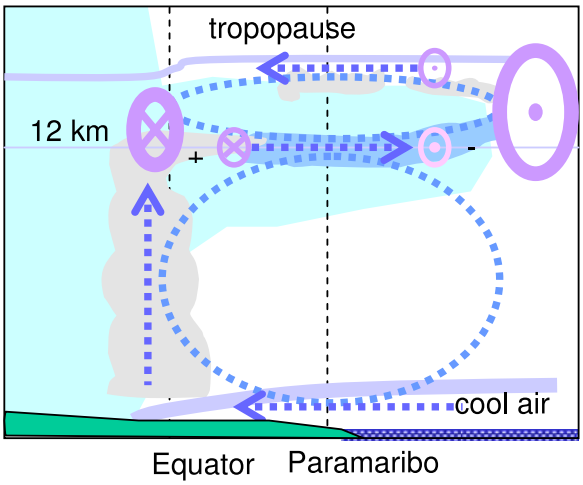

Figure 6. Schematic illustration of the meridional circulation, when the ITCZ lies to the south of Paramaribo. A negative PV zone (light blue shaded) in the upper troposphere develops when the STJ (westerly, circle with dot) migrates close to the equator with an easterly jet (circle with cross), starting a cellular flow (blue dotted lines) that transports moisture (dark blue shaded) and cirrus (grey).

and depicted in their Figure 5d. This type of inertial instability flow lasts for a couple of days, which is consistent with the inertial frequency of this latitude ($\sim 1/f$). After this period the horizontal wind shear is largely eliminated and the PV becomes positive again. The meridional exchange will then cease or change direction, which again allows zonal wind shear to build up near the equator, leading to inertial instability and so forth.

[17] The above situation occurs when the ITCZ lies south of Paramaribo. When the ITCZ is at its northernmost boundary along 10°N, a situation arises similar to the one found by *Fu03* on their ship campaign in the equatorial eastern Pacific. As discussed in section 1, the detrained moist air from the ITCZ creates an easterly jet through the thermal wind relation as the humid layer journeys southward, which again spreads the humidity and UTI downstream along the equator. Hence the UTI is a widespread feature, and *Fu03* suggest that it can often constitute the bottom of the TTL. From Figure 5d we see that easterlies indeed dominate in the UT when the ITCZ is to the north (August–October). Also here we see a broad layer directly above 10 km where minimum lapse rates are encountered (Figure 5c), which is usually the layer where moist outflow occurs and thus supports the view of strong radiative cooling. An important additional element in the present study is however the occurrence of cirrus, which most often is encountered within the TTL above the moist layer. It seems therefore that the cirrus events in the TTL do not significantly change the strong cooling characteristics of the moist layer below. From radiative transfer calculations performed for humid layers at various height levels, *Fu03* found that the cooling rate within (and warming rate directly underneath) the moist layer decreases with height, mainly due to the lower water vapor number density. Looking at the lapse rates calculated directly from radiosondes (Figure 3c), there is some evidence that UTIs are created at the top of observed cirrus clouds (Figure 3a), which shows that they too cool radiatively and create UTI's at height levels close to the tropopause (i.e., for 31 October, 5 November, and 16 November; at or above 15 km height). Cirrus may even enhance the longwave and net cooling at the top of the moist outflow layer.

[18] Reverting again to an ECMWF analysis case, now for 11 November 2004, Figure 8a shows an easterly jet centered at 5°N, 200 hPa, which could be the result of the southward transport (Figure 8c, area marked with a "B") of humid air outflow to the north (Figure 8d). As the easterly jet develops near the equator, one would however expect that inertial instability also starts to play a role, as it did in the previous case with the STJ. For an easterly jet however PV values on the equator side of the jet remain positive, as the local vorticity ($-\partial u/\partial y$, neglecting $\partial v/\partial x$) is now positive. Only pole ward of the easterly jet can negative values develop, as can be seen to happen in Figure 8b, in the "B" area. In this negative PV zone inertial unstable flow will oppose the existing flow, as it tries to transport easterly momentum northward and cut off the southward transport of moist air, as can be seen to happen two days later (Figures 8e–8h). Note however that the easterly jet has strengthened and lowered its altitude in this period, which must be due to another cause than the thermal wind relation proposed by Fu03, as this occurs in a dry layer where there is no southward transport. Eventually the center of the easterly will shift toward the equator as its poleward side is eroded away by northward transport through inertial instability (not shown).

[19] If the thermal wind relation described above plays an important role in establishing an easterly jet south of an ITCZ in its northernmost position, one would expect a similar but reverse role for when the ITCZ is at its southernmost position and transports moist air northward; as depicted in Figure 6. Returning to the earlier scenario centered around Figure 7, we see that indeed westerlies dominate in the upper troposphere (Figure 5d), now supposedly due to a reverse latitudinal temperature gradient in the moist outflow layer which cools progressively as it is transported northward. If this is indeed the case, the westerly STJ would be fed by the thermally induced wind, which again would raise the horizontal wind shear and help maintain a negative PV field. Also for this instance the inertial unstable flow will counteract the background flow, as it tends to transport the created westerly momentum southward again, as it is deflected and accelerated to the right by coriolis. Hence one would expect that northward flow of moist air with an easterly momentum would be intermitted by southward transport of air with a strong westerly momentum. Such an alternation is evident in meridional wind (Figure 5e) and a closer inspection reveals that the westerly wind (Figure 5d) during the monsoon period is modulated with an easterly (or less westerly) component that has a similar structure as the meridional southerly wind field of Figure 5e.

4.2. Climatological Features of Tropical South America

[20] The interaction between the two mechanisms, inertial instability and thermal wind flow near the equator, was the

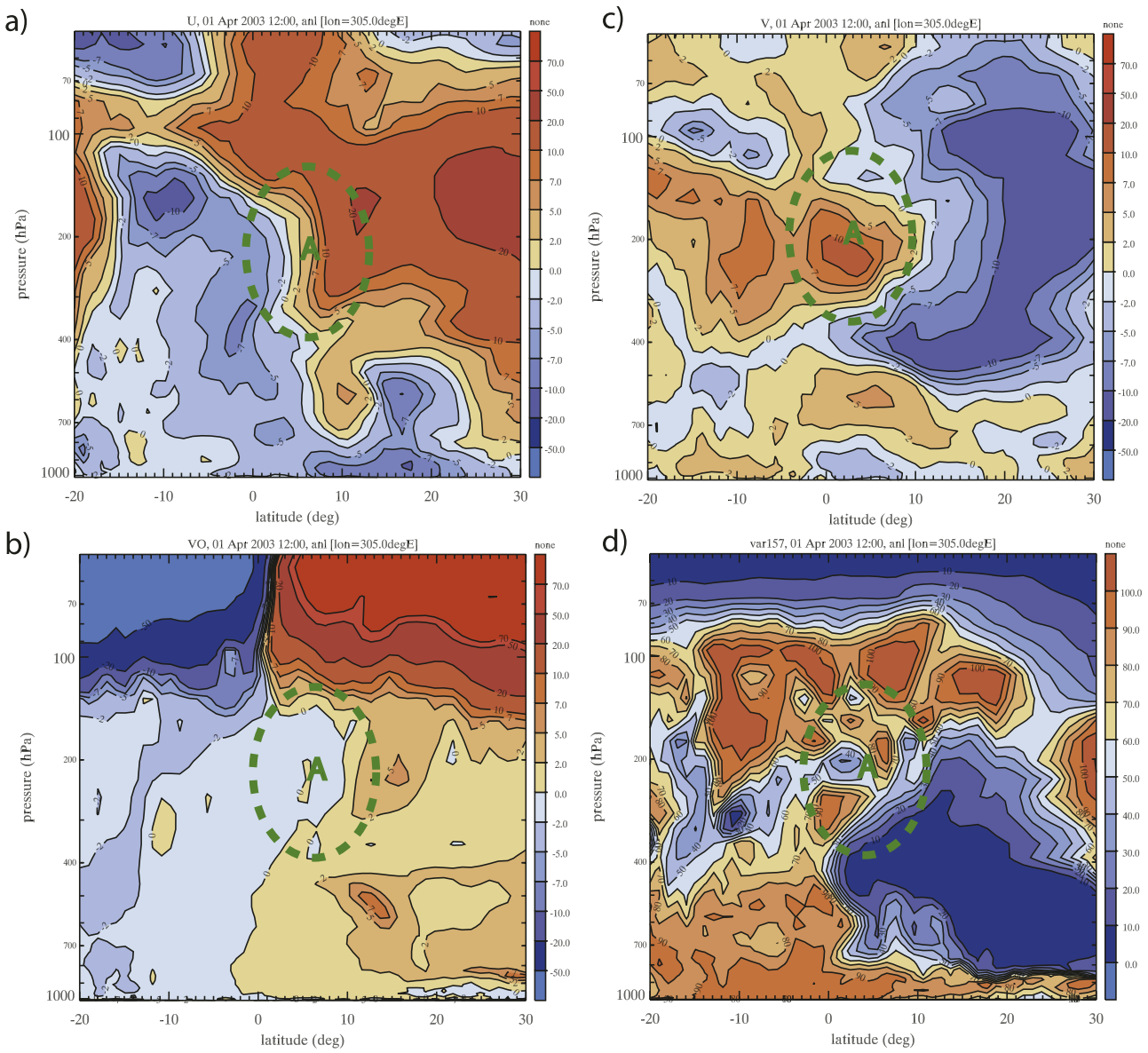

Figure 7. ECMWF pressure-latitude cross sections at the longitude of Paramaribo (55°W), showing zonal wind (a), potential vorticity or PV (b), meridional wind (c) and relative humidity (d) for 1 April 2003.

focus around which the previous analysis was formed. Also, for the sake of clarity, the scope was limited to the processes in close vicinity to the ITCZ and Paramaribo. In reality of course many other processes coexist and mingle with the studied ones. We will now present some of the background climatological features of tropical South America. This will then be followed by a 3-D back-trajectory analysis, in which the origin of air mass in the UT above Paramaribo are determined, and the route of the trajectories are discussed in terms of all the considered transport processes.

[21] For the case study in mid November 2004, with the ITCZ to the north, one can see from Figures 8d and 8h that there is also deep convection occurring south of the equator, around 10°S. This is because the ITCZ at this stage has already reached the northernmost point of the South American continent in Venezuela and Colombia. Moist air is now transported with a climatologically well-known low-level jet (LLJ), along the eastern slopes of the Andes, to the south where early summer heating has created a thermal low over land. So, even though Suriname is still experiencing its long dry season, the wet season has already started land inward to the south. Suriname therefore lies sandwiched between two convective regions to the north and south, as can be seen in the geographical overview of ECMWF convective precipitation in Figure 9b. In December, the southward migrating ITCZ has reached the coast of Suriname and within two months crosses over Paramaribo, which is the duration of the short wet season. *Zhou and Lau* [1998] showed that the wet season in South America does indeed have monsoon characteristics, and that the South American Summer Monsoon (SASM) development can be divided into five stages. At the monsoon onset there are two UT

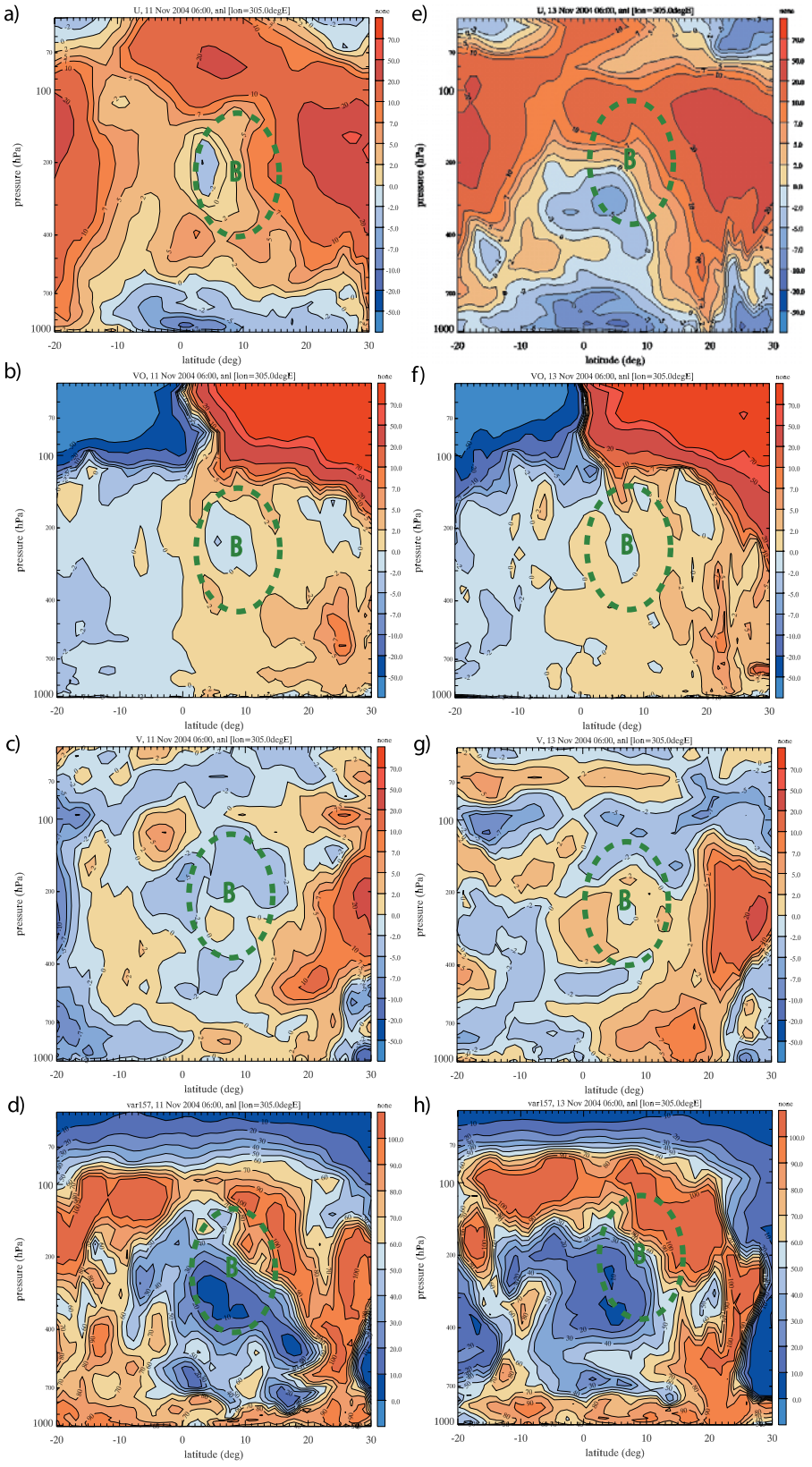

Figure 8. ECMWF pressure-latitude cross sections for 11 November 2004 (a–d) and 13 November 2004 (e–h) at the longitude of Paramaribo (55°W) showing zonal wind (Figures 8a and 8e), potential vorticity or PV (Figures 8b and 8f), meridional wind (Figures 8c and 8g) and relative humidity (Figures 8d and 8h).

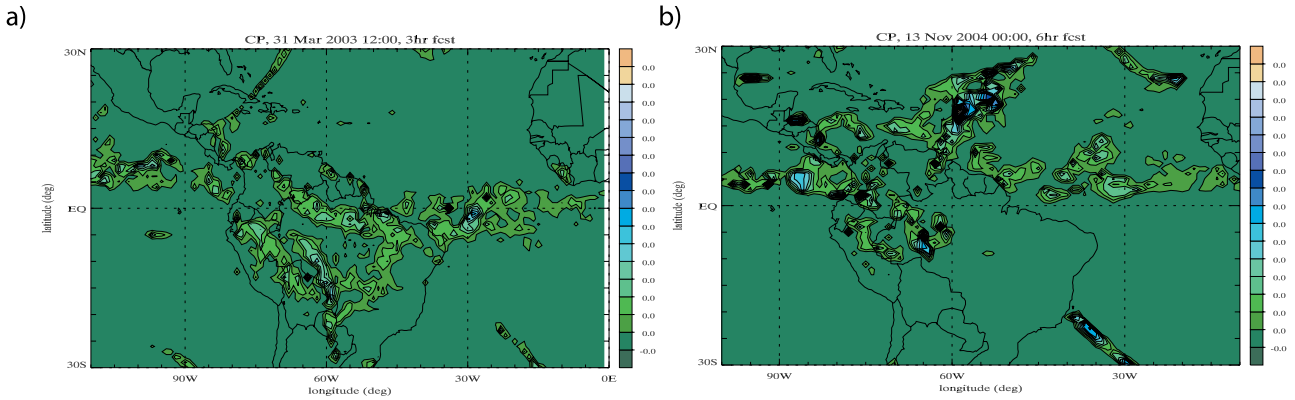

Figure 9. ECMWF convective precipitation fields, for (a) 31 March 2003 during the short dry season when the ITCZ lies to the south of Suriname and (b) 13 November 2004 during the long dry season when the ITCZ lies to the north of Suriname.

westerly jets, subtropical and midlatitudinal, over South America, driven largely by the dominant north–south temperature gradients between tropics and extratropics. As the continent warms in summer, the dominant temperature gradient becomes east–west, between the South American continent and the surrounding ocean. Transport in the UT, where the Bolivian High has developed itself, then becomes decidedly meridional because of the thermal wind relation, causing cross-equatorial transport to the east and a single jet to the south. The Bolivian High develops as a result of deep convection over the heated Altiplano Plateau. Also, further to the southeast the South Atlantic Convergence Zone (SACZ) starts to form, bringing rain to subtropical South America. Around February–March the ITCZ has reached its southernmost position, just past the equator over the Atlantic Ocean. This coincides with the short dry season in Suriname when most deep convection lies to the south, as can be seen from ECMWF convective precipitation map for 31 March 2003, in Figure 9a. After this, a gradual retreat of heavy precipitation follows the ITCZ back northward over Suriname, bringing the long wet season that lasts 4 months (April–July). During this stage precipitation in the subtropics (southern Brazil, Argentine) decreases and a double jet as in the premonsoon era develops again.

4.3. Back-Trajectory Analysis

[22] ECMWF 5-day back-trajectories were calculated for the Snow White launches listed in Table 1, starting at the pressure levels where cirrus clouds were detected. The 3-D trajectories were calculated over a five-day period using the TRAJKS model [*Scheele et al.*, 1996] of the KNMI, whilst keeping track of the parameters specific humidity, cloud fraction, cloud ice content, convective precipitation amount and boundary layer height. The trajectories were only calculated from those pressure levels where the Snow White cirrus coincided with ice saturated or near-saturated ECMWF humidity values; back to the point which either marks a deep convection event or the endpoint of the trajectory. If convective precipitation would coincide with an increase in cloud ice content and cloud fraction at the height of the trajectory, it was considered to be the origin point of the cirrus. This origin point was compared with infrared images coming from METEOSAT (full Earth view every half hour, used for the pilot study campaign, from October–November 2004) and from GOES8 and GOES20 (NH half-disk view every 6 hours, respectively over the periods October 2002–April 2003 and May 2003–March 2004,). Within the accuracy allowed by such a method, these points were found to agree well with low OLR (outward longwave radiation) or Cumulonimbus events. Figures 10 and 12 present the geographical distribution of these points of origin, respectively for the long dry period with the ITCZ to the north (August–November), and for the SASM period with the ITCZ to the south or overhead (January–June). A further subdivision is made by height intervals: 10–14 km versus 14 km to tropopause, respectively for the a- or b-part of the figures. This layer division is made to distinguish between cirrus transported at typical height levels of the upper branch of the Hadley cell (or the strongly cooled moist layer, as discussed earlier), versus cirrus transported into the TTL above this layer by means of other processes. A solid dot indicates where the back-trajectory was cut off by a deep convective outflow event, whereas an open circle shows the end point of the back-trajectory, indicating no deep convective source along the route.

4.3.1. ITCZ to the North

[23] In the long dry season, we see from Figure 10a that most cirrus within the lower UT layer comes either directly from the ITCZ to the north, or from deep convection events to the south as described in the onset phase of SASM earlier. This seems to point either to transport with the Hadley cell from an ITCZ source, or to transport in the UT with the anticyclonal circulation associated with the outflow over deep convection clusters, as discussed earlier. Figure 10b shows that for the higher TTL layer, less cirrus events occur than in the layer directly below. The source regions are similar to those for the lower layer, suggesting that the upper Hadley circulation is quite deep and that deep convection events inland penetrate up to various heights, also into the TTL. A closer inspection of the trajectory routes however reveals that the transport mechanisms discussed in section 4a can also be recognized. Figure 11 shows typical back-trajectories that are encountered during

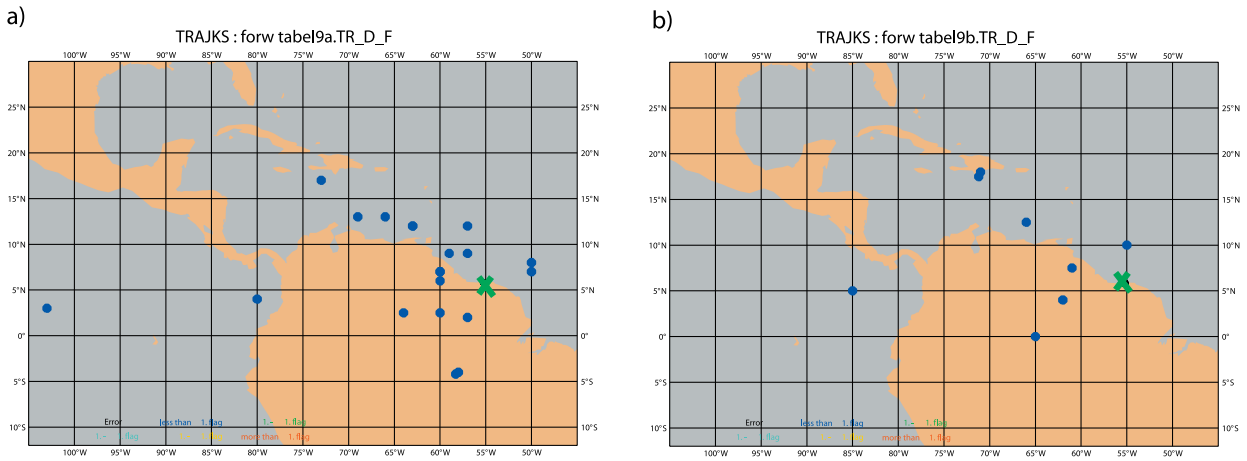

Figure 10. Points of origin of cirrus clouds detected over Paramaribo (green cross) between (a) height interval 10–14 km and (b) 14–18 km (tropical tropopause layer (TTL)); using 5-day ECMWF back-trajectories over the period August–November (long dry season for Suriname, compare with Table 1). Solid blue dots indicate the convective origin of the detected cirrus (see text).

the long dry period, now calculated for one specific day (Snow White launch nr. 27, on 16 November 2004) from 34 trajectory starting points over Paramaribo equally divided over the interval 10–18 km (i.e., each 250 m). Shown are the pressure evolution of the trajectories (Figure 11a), their convective precipitation history (Figure 11b), and the cloud fraction development within the trajectory grid boxes (Figure 11c). Starting from the lowest height levels (the blue and green trajectories of. Figure 11a), we see that the trajectories mostly come from the north via an eastward loop, arriving above Paramaribo from the southeast. Three of these trajectories show convective precipitation (Figure 11b) around 13°N where the ITCZ is located, combined with an increase in cloud cover (Figure 11c). The cloud cover then rapidly decreases as transport sinks to a lower height level (yellow to light blue) and continues southeastward. The gradual turn of the trajectory to the west would then be in agreement with the concept of an easterly developing as the moist layer cools radiatively, as discussed earlier. Around 5°N the flow turns northward, which is about at the same date, height and latitude (but not longitude) of the negative PV zone encountered in Figure 8b, on the north side of the easterly jet. Inertial instability flow in this zone would act to transport easterly momentum northward, which would explain the northward turn of the trajectory here. At this stage also convective precipitation occurs below (Figure 11b), but this is seen to have no effect on the cloud cover at the trajectory height.

[24] For the higher height interval of 12–14.5 km (the yellow trajectories) we see on average a completely different moisture source, lying land inward where most convective precipitation occurs between 0–5°S and 60–65°W, and cloud cover at trajectory height increases correspondingly. The moisture is then transported at high altitude across the equator with an UT anticyclonal circulation, as discussed earlier in this section. Before these trajectories reach Paramaribo we see an increase in cloud cover occurring even though there is no convective precipitation below, indicating cloud nucleation through a rising motion (yellow to red transition, Figure 11a, at 5°S 57°W).

[25] For the highest height interval above 14.5 km (red trajectories) we distinguish yet another moisture source, directly to the west and northwest of Suriname where the ITCZ touches the northernmost coast of South America. Clearly here the deepest convection penetrating right into the TTL as cirrus cloud cover increases to over 80% before it is advected eastward to Paramaribo, deflected by coriolis to the right as it travels along.

4.3.2. ITCZ to the South or Overhead

[26] Not too many Snow White sondes were launched during the wet seasons in Paramaribo when the ITCZ is overhead, only 3 soundings during the long wet period (April–July) and one unsuccessful sounding during the short wet period; as given in Table 1. The short dry period in February–March when the ITCZ lies to the south is better sampled with 7 soundings, but still not enough to obtain good statistical insights. Still, the origin points of cirrus detected during the SASM do show some interesting features. With the same height distinction used earlier, we see in Figure 12a that all cirrus detected from 10–14 km come from the south, where satellite pictures and ECMWF precipitation maps (compare with Figure 9a) confirm deep convective events in a broad band over the Amazon area. Again a solid dot indicates a convective source where cloud cover increased at that location along the trajectory. The cirrus events in Figure 12a therefore seem to be directly transported with the Hadley cell from deep convective outflow associated with the ITCZ. For the height interval above that (14 km to tropopause) we see only a few convective moisture sources, now distributed to the south, west and northwest, whereas the other back-trajectories encountered no precipitation event and hence an open circle denotes their origin 5 days earlier.

[27] Again, one day is selected that exhibits typical trajectories encountered for this period: on 17 March 2004. Similar to the previous case, the pressure evolution, convective precipitation history, and cloud fraction devel-

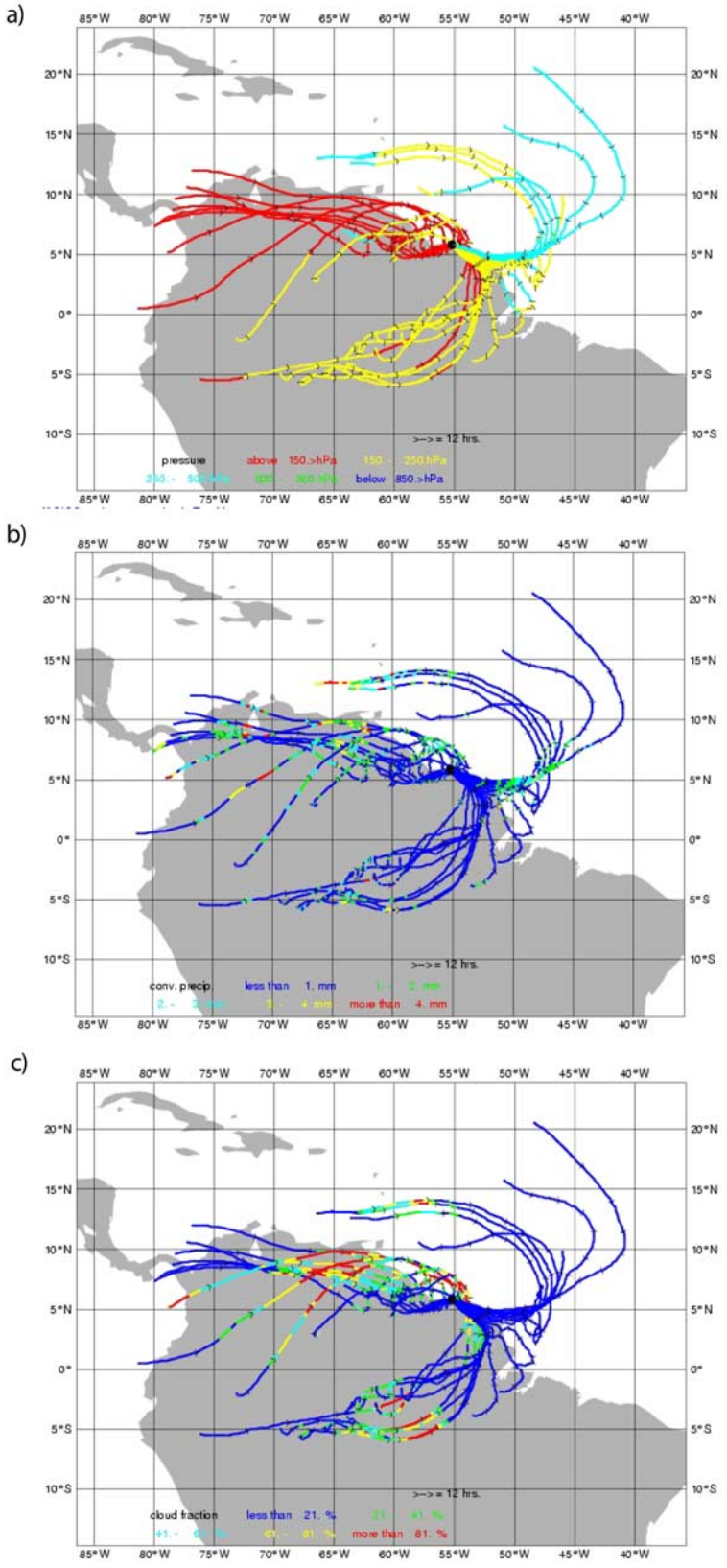

Figure 11. ECMWF 3-D five-day back-trajectories for 16 November 2004 showing (a) pressure history (red: above 140 hPa, yellow: 140–206 hPa, light blue: 206–272 hPa, green: 272–338 hPa, dark blue below 338 hPa), (b) convective precipitation in mm (from dark blue: <1 mm to red: >4 mm, (c) cloud cover fraction at the height of the trajectory (from dark blue: <21%, to red: >85%). Black cross lines indicate a 12-hour interval.

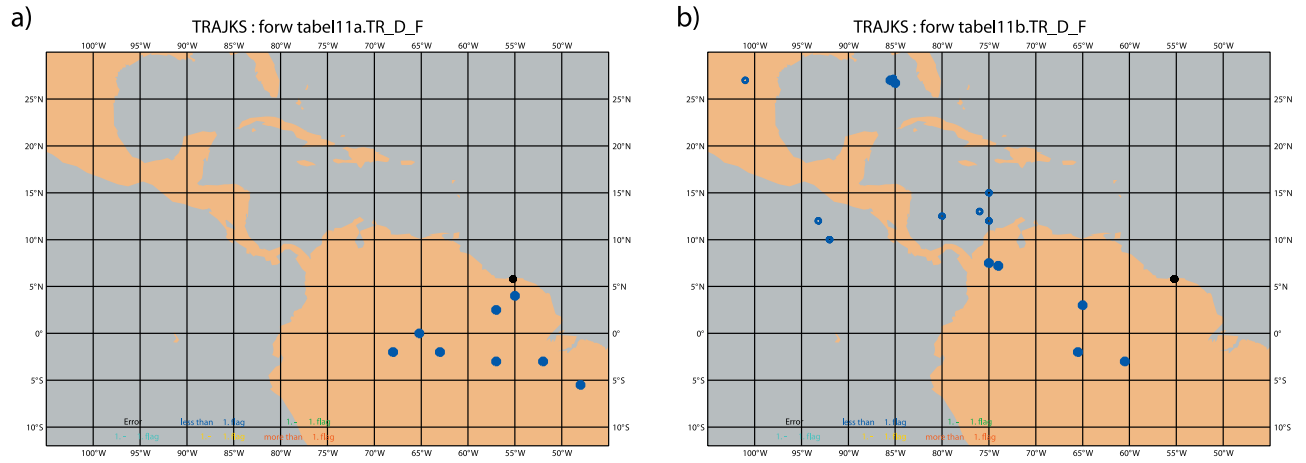

Figure 12. Points of origin of cirrus clouds detected over Paramaribo (black dot) between (a) height interval 10–14 km and (b) 14–18 km (TTL); using 5-day ECMWF back-trajectories over the period January–June (monsoon period, compare with Table 1). Solid blue dots indicate a convective origin (see text); open blue circles indicate the endpoint of trajectory without encountering deep convection.

opment for 34 trajectories are shown in Figure 13. Noticeable this time is that most convective precipitation encountered by the trajectories occurs south in the Amazon area (Figure 13b). Other convective areas are those associated with the ITCZ over the Atlantic and East Pacific Ocean. In its mature stage of development, the SASM now has the characteristic Bolivian High fully developed in the UT above the Altiplano Plateau (~18°S 60°W). Thus the anticyclone has shifted southward compared to the November case discussed earlier, when the center lied above the Amazon area just south of the equator. Therefore moist outflow from deep convection over central Brazil (around 10°S 50°W in Figure 13b, corresponding with light blue to yellow trajectories in Figure 13a) is now transported northward by the Bolivian High, and consequently feeds in to the easterly jet at the equator where more precipitation occurs associated with the ITCZ. Inertial instability in the UT (as discussed earlier) will accelerate easterly momentum near the equator northward as we can see happens with the trajectories near and north of the equator, west of 60°W. If radiative cooling of the moist outflow layer is dominant, this northward transport will lead to a thermal wind westerly which can explain the gradual eastward bend of the trajectories as they proceed northward. As the air parcels reach their northernmost point, they ascends into the TTL (yellow to red transition around 7°N 65°W in Figure 13a) and flow southward again. This agrees with a rise into the subcell above the Hadley cell, due to the vertically stacked cellular flow resulting from inertial instability, as discussed earlier. The ascent is accompanied by an increase in cloud cover (Figure 13c, same location) due to adiabatic cooling. The cloud cover generated in this way maintains itself until it reaches Paramaribo as cirrus in the TTL.

[28] Apart from this, it is evident from the remaining trajectories that cirrus can come from deep convection over water, to the west in the Caribbean Sea and even East Pacific (Figure 13b). Another noticeable feature is that the higher trajectories (red, in Figure 13a) have mostly westerly momentum and thus seem to be part of the STJ until they are deflected to the right by coriolis. This latter explanation of coriolis deflection can of course also explain many of the features attributed to more complex mechanisms in the discussions before. A more careful and detailed study is therefore needed to assess the contribution of each, as this is beyond the scope of this paper.

5. Discussion and Conclusions

[29] Upper tropospheric humidity and cirrus in ECMWF operational analyses above Paramaribo are found to agree quite well with both Snow White hygrometer observations (October 2002 to November 2004) and lidar backscatter profiles (pilot study period, October–November 2004) performed at this spot. Also ECMWF temperature and wind compare well with the radiosonde observations over Paramaribo, for the whole observation period (September 1999 to present) in general, and for the pilot study period in particular. This justifies the use of ECMWF data for a more detailed analysis on the origin and transport dynamics of cirrus over Paramaribo. A first notable feature is that the height of cirrus occurrence is in phase with the height of the cold point tropopause, with maximum values in January–March (height ~18 km) about 2 km above the minimum values in June–August. This can be related to an intensified Brewer-Dobson circulation in NH winter, causing a colder and higher tropopause, and lower saturation values over ice so that cirrus can form more easily.

[30] Most of the time, cirrus over Paramaribo is advected with northerly flow, even when the ITCZ lies to the south of Paramaribo. During NH winter, the southward flow that transports cirrus clouds near tropopause levels could be the result of inertial instability flow, as found by *Fo03* for the UT over Paramaribo. The negative PV that then prevails in the UT is caused by the close proximity of the STJ to the equator, which results in a vertically stacked cellular flow pattern, between the equator and the edge of the negative PV field, in the form of a subcell on top of the Hadley cell.

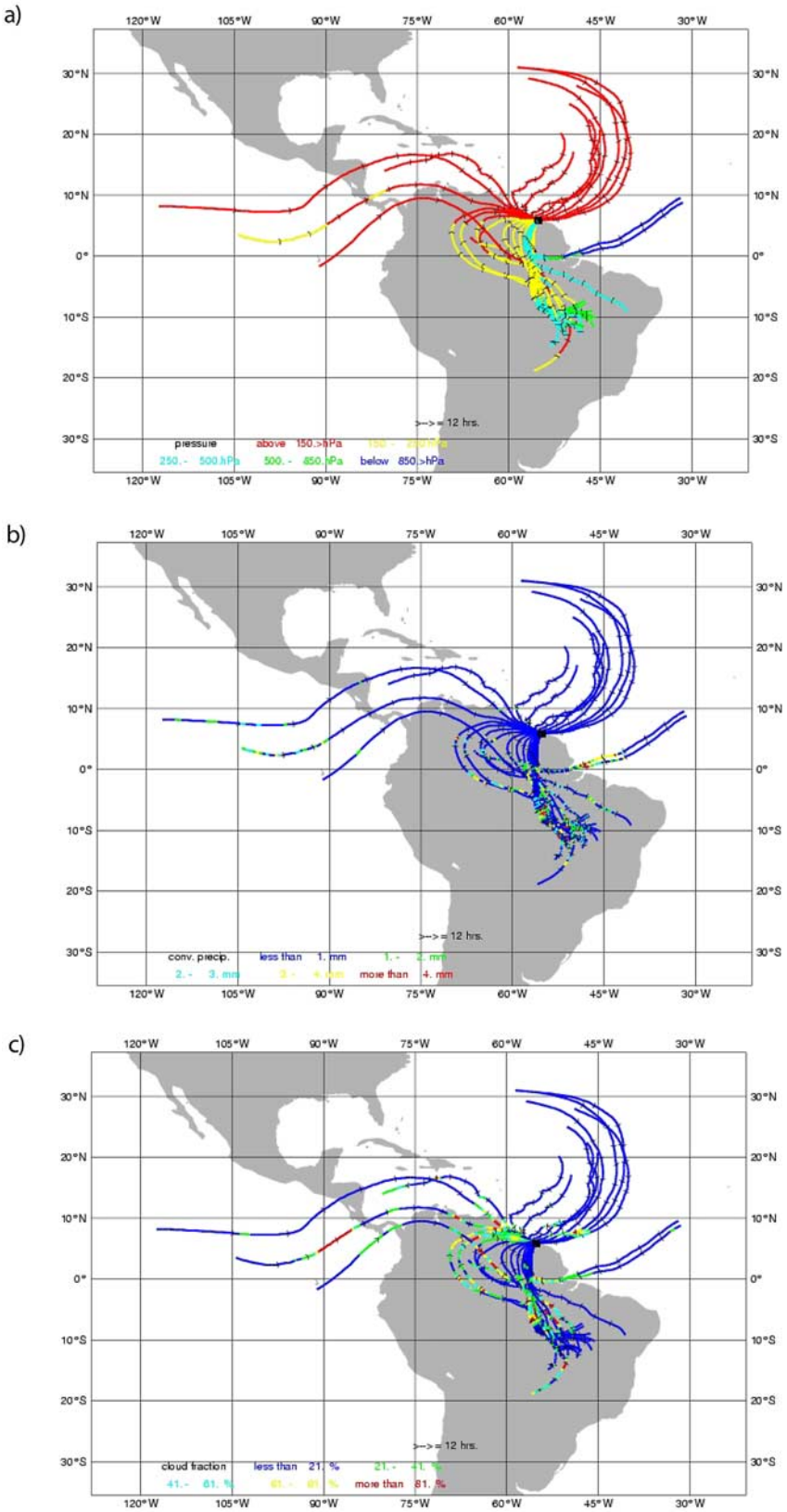

Figure 13. ECMWF 3-D five-day back-trajectories for 17 March 2004 showing (a) pressure history (red: above 150 hPa, yellow: 150–250 hPa, light blue: 250–500 hPa, green: 500–850 hPa, dark blue below 850 hPa), (b) convective precipitation in mm (from dark blue: <1 mm to red: >4 mm, (c) cloud cover fraction at the height of the trajectory (from dark blue: <21%, to red: >85%). Black cross-lines indicate a 12-hour interval.

The subcell generated in this way can thus lift the moist air transported in the upper Hadley branch upward and recirculate the condensed air back south toward the equator. The Hadley cell and subcell respectively act to transport easterly momentum from the equator northward, and westerly momentum from the STJ southward, until the zonal wind shear is alleviated and the negative PV field disappears.

[31] Another dynamical mechanism that seems to play an important role corresponds with the formation of a jet through the thermal wind relation, when moist air is cooled radiatively while being transported in the UT, as first presented by *Fu03* on the basis of shipboard observations in the tropical eastern Pacific. Hence moist air in the UT being transported southward/northward, corresponding with an ITCZ to the north/south, will cool radiatively and produce a UTI and an easterly/westerly jet that spreads the UTI downstream. Easterly winds indeed dominate the UT over Paramaribo when the ITCZ is to the north, as westerly winds do when the ITCZ is to the south. In the latter case, inertial instability in the UT is deep and widespread enough to allow vertically stacked flow, as predicted from theory for zonal symmetric conditions. This allows the westerly momentum, generated through the thermal wind relation, to be transported back southward in a higher layer by the subcell. When the ITCZ is to the north, negative PV zones are smaller in horizontal and vertical extent, and therefore do not seem to allow the same vertically stacked flow. Thus southward transport of moist air (creating an easterly jet) is then inhibited by counteracting inertial unstable flow (transport of easterly momentum northward) at the same height levels. This could explain the more steady flow regime in the UT during SASM, when the vertically stacked cells from inertial instability do not oppose the thermal wind flow (northward transport of moist air) at the same height level.

[32] ECMWF back-trajectories, in combination with satellite infrared pictures, indicate that other dynamical features also play an important role in the transport and formation of cirrus. From August–November, during the long dry season in Suriname, cirrus can often be traced to the ITCZ that then lies to the north. However, from end October onward, cirrus can also be traced to deep convective events inland to the south. This is because the ITCZ has then reached the northernmost point of the South American continent and moist air flows with a low-level jet along the eastern slopes of the Andes southward bringing deep convection over the Amazon area and beyond. Anticyclonal circulation in the UT above centers of deep convection then transports the moist outflow northward over Paramaribo in the form of cirrus clouds. As the SAMS develops further and the ITCZ moves over Paramaribo to its southernmost position near the equator, the UT anticyclone strengthens and shifts southward with the center of deep convection, where it is now known as the Bolivian High. The northern edge of the Bolivian High feeds into an easterly jet in the UT over the equator. The easterly jet, in combination with the equatorward shifting STJ to the north, gives rise to a strong horizontal wind shear and prevalent negative PV fields in the UT directly north of the equator, with the consequences for inertial unstable flow sketched above.

[33] This paper has focused on the contribution of the transport mechanisms proposed by *Fu03* and *Fo03*, to understand the formation and advection of cirrus. Some essential features from the observations could be explained in this context, but there is clearly need for a subsequent study that theoretically or numerically validates and quantifies the contribution of these individual processes, and also determines the role of other processes not considered in this study. For example, the signature of more familiar meteorological features in the tropics like the passage of a trough associated with the subtropical jet, or of tropical Kelvin and Rossby-gravity waves, could then be compared with the inertial instability features to assess the differences and similarities.

[34] **Acknowledgments.** The authors wish to thank the operator team of Paramaribo station for their excellent work and dedication throughout the years. Paul de Valk is acknowledged for the preparation of METEOSAT images that were used in this study. Also, we thank the reviewers for valuable comments to improve the paper content. The ground-receiving equipment for the Snow White hygrometer were provided by a project, Soundings of Ozone and Water in the Equatorial Region (SOWER). The present study, as well as the pilot study campaigns, is financed by the European Union through the STAR project (Support for Tropical Atmospheric Research), EU project SSA506651.

References

Dunkerton, T. J. (1981), On the inertial instability of the Equatorial middle atmosphere, *J. Atmos. Sci.*, *38*, 2354–2364.

Fortuin, J. P. F., H. M. Kelder, M. Sigmond, R. Oemraw, and C. R. Becker (2003), Inertial instability over Suriname during the South American Monsoon, *Geophys. Res. Lett.*, *30*(9), 1482, doi:10.1029/2002GL016754.

Fueglistaler, S., H. Wernli, and T. Peter (2004), Tropical troposphere-to-stratosphere inferred from trajectory calculations, *J. Geophys. Res.*, *109*, D03108, doi:10.1029/2003JD004069.

Fujiwara, M., S.-P. Xie, M. Shiotani, H. Hashizume, F. Hasebe, H. Vömel, S. J. Oltmans, and T. Wanatabe (2003a), Upper-tropospheric inversion and easterly jet in the tropics, *J. Geophys. Res.*, *108*(D24), 4796, doi:10.1029/2003JD003928.

Fujiwara, M., M. Shiotani, H. Hashizume, F. Hasebe, H. Vömel, S. J. Oltmans, P. W. Ruppert, T. Horinouchi, and T. Tsuda (2003b), Performance of the Meteolabor "Snow White" chilled-mirror hygrometer in the tropical troposphere: Comparisons with the Vaisala RS80 A/H-Humicap sensors, *J. Atmos. Oceanic Technol.*, *20*, 1534–1542.

Haynes, P. H., C. J. Marks, M. E. McIntyre, T. G. Shepherd, and K. P. Shine (1991), On the "downward control" of extratropical diabatic circulations by eddy-induced mean zonal forces, *J. Atmos. Sci.*, *48*, 651–678.

Heymsfield, A. J., L. M. Miloshevich, C. Twohy, G. Sachse, and S. Oltmans (1998), Upper tropospheric relative humidity observations and implications for cirrus ice nucleation, *Geophys. Res. Lett.*, *25*(9), 1343–1346.

Highwood, E. J., and B. J. Hoskins (1998), The tropical tropopause, *Q. J. R. Meteorol. Soc.*, *124*, 1579–1604.

Hitchman, M. H., C. B. Leovy, J. C. Gille, and P. B. Bailey (1987), Quasi-stationary zonally asymmetric circulations in the equatorial lower mesosphere, *J. Atmos. Sci.*, *40*, 2219–2236.

Hyland, R. W., and A. Wexler (1983), Formulations for the thermodynamic properties of the saturated phases of water from 173.15 K to 473.15 K, *ASHRAE Trans.*, *89*(2A), 500–519.

Immler, F., and O. Schrems (2002), Determination of tropical cirrus properties by simultaneous lidar and radiosonde measurements, *Geophys. Res. Lett.*, *29*(23), 2090, doi:10.1029/2002GL015076.

Immler, F., K. Krüger, S. Tegtmeier, M. Fujiwara, G. H. L. Verver, P. Fortuin, and O. Schrems (2007), Cirrus clouds, humidity, and dehydration at the tropical tropopause observed in Paramaribo, Suriname (5.8°N, 55.2°W), *J. Geophys. Res.*, *112*, D03209, doi:10.1029/2006JD007440.

Jensen, E., and L. Pfister (2005), Implications of persistent ice supersaturation in cold cirrus for stratospheric water vapor, *Geophys. Res. Lett.*, *32*, L01808, doi:10.1029/2004GL021125.

Jensen, E. J., L. Pfister, A. S. Ackerman, A. Tabazadeh, and O. B. Toon (2001), A conceptual model of the dehydration of air due to freeze-drying by optically thin, laminar cirrus rising slowly across the tropical tropopause, *J. Geophys. Res.*, *106*, 17,237–17,252.

Luo, Z., and W. B. Rossow (2004), Characterizing tropical cirrus life cycle, evolution, and interaction with upper-tropospheric water vapor using Lagrangian trajectory analysis of satellite observations, *J. Clim.*, *17*, 4541–4563.

Sato, K., and T. J. Dunkerton (2002), Layered structure associated with low potential vorticity near the tropopause seen in high-resolution radiosondes over Japan, *J. Atmos. Sci.*, *59*, 2782–2800.

Scheele, M. P., P. C. Siegmund, and P. F. J. van Velthoven (1996), Sensitivity of trajectories to data resolution and its dependence on the starting point: in or outside a tropopause fold, *Meteorol. Appl.*, *3*, 267–273.

Seidel, D. J., R. J. Ross, J. K. Angell, and G. C. Reid (2001), Climatological characteristics of the tropical tropopause as revealed by radiosondes, *J. Geophys. Res.*, *106*, 7857–7878.

Verver, G. H. L., M. Fujiwara, C. R. Becker, P. Dolmans, and J. P. F. Fortuin (2006), Performance of the Vaisala RS80 A/H and RS90 Humicap sensors and the Meteolabor Snow White chilled-mirror hygrometer in Paramaribo, Suriname, *J. Atmos. Oceanic Technol.*, *23*(11), 1506–1518.

Vömel, H., M. Fujiwara, M. Shiotani, F. Hasebe, S. J. Oltmans, and J. E. Barnes (2003), The behavior of the Snow White chilled-mirror hygrometer in extremely dry conditions, *J. Atmos. Oceanic Technol.*, *20*, 1560–1567.

Zhou, J., and K.-M. Lau (1998), Does a monsoon climate exist over South America?, *J. Clim.*, *11*, 1020–1040.

C. R. Becker, Meteorological Service Suriname, Magnesiumstraat 41, Paramaribo, Suriname.

J. P. F. Fortuin, Road and Hydraulics Engineering Institute of the Netherlands Public Works Department, P.O. Box 5044, 2600 GA, Delft, Netherlands. (p.fortuin@dww.rws.minvenw.nl)

M. Fujiwara, Graduate School of Environmental Earth Science, Hokkaido University, Sapporo, Hokkaido 060-0810, Japan.

F. Immler and O. Schrems, Alfred Wegener Institute for Polar and Marine Research, Am Handelshafen 12, D-27570 Bremerhaven, Germany.

H. M. Kelder, M. P. Scheele, and G. H. L. Verver, Royal Netherlands Meteorological Institute (KNMI), P.O. Box 201, 3730 AE De Bilt, Netherlands.